SORET AND HEAT SOURCE EFFECTS ON MHD FLOW OF A VISCOUS FLUID IN A PARALLEL POROUS PLATE CHANNEL IN PRESENCE OF SLIP CONDITION

Malapati VENKATESWARLU[*†], Meduri PHANI KUMAR[†]

The heat and mass transfer characteristics of the unsteady viscous, income-pressible and electrically conducting fluid flow past a porous parallel plate channel are taken into account in this paper. Based on the pulsatile flow nature, exact solution of the governing equations for the fluid velocity, temperature and concentration are obtained by using two term perturbation technique. The expressions of skin friction, Nusselt number and Sherwood number are also derived. The numerical values of fluid velocity, temperature and concentration are displayed graphically whereas those of shear stress, rate of heat transfer and rate of mass transfer at the plate are presented in tabular form for various values of pertinent flow parameters.

Keywords: MHD fluid, Porous medium, Heat source, Parallel plate channel.

Nomenclature:

h	**distance between two parallel plates**	H	non- dimensional heat source
B_o	**uniform magnetic field**	j_w	mass flux
C	**species concentration**	K	permeability of porous medium
C_f	**skin-friction coefficient**	K_r^*	dimensional chemical reaction parameter
C_1	**species concentration at the heated wall**	Kr	non-dimensional chemical reaction parameter
C_o	**species concentration at the cold wall**	K_T	thermal conductivity of the fluid
c_p	**specific heat at constant pressure**	M	magnetic parameter
Da	**Darcy parameter**	Nu	Nusselt number
D_m	**chemical molecular diffusivity**	n	frequency of oscillation
Gm	**Solutal Grashof number**	Pr	Prandtl number
Gr	**thermal Grashof number**	Q_o	dimensional heat source
g	**acceleration due to gravity**	q_w	heat flux
U	**A scaled velocity**		
Sc	**Schmidt number**	ω	A scaled frequency
Sh	**Sherwood number**	ϕ	A scaled concentration

[1]Assistant Professor, Department of Mathematics, V. R. Siddhartha Engineering College, Kanuru, Vijayawada, Andhra Pradesh, India, PIN: 520 007. Email: mvsr2010@gmail.com
[2]Assistant Professor, Department of Mathematics, Vellore Institute of Technology, Amaravathi, Andhra Pradesh, India, PIN: 522 237. Email: phanikumarmeduri@gmail.com

Sr	**Soret number**	ϕ_1	dimensional cold wall slip parameter
T	**fluid temperature**	ϕ_2	dimensional heated wall slip parameter
T_m	**mean temperature of the fluid**		
T_1	**fluid temperature at the heated wall**	ρ	fluid density
T_o	**fluid temperature at the cold wall**	σ_e	electrical conductivity
t	**dimensional time**	τ	non dimensional time
u	**fluid velocity in $x-$ direction**	τ_w	shear stress
v	**fluid velocity in $y-$ direction**	ψ	A scaled coordinate
Greek Symbols		η	A scaled coordinate
		θ	A scaled temperature
β_c	**coefficient of concentration expansion**	γ	non-dimensional cold wall slip parameter
β_T	**coefficient of thermal expansion**	σ	non-dimensional heated wall slip parameter
ν	**kinematic coefficient of viscosity**		

1. Introduction

The study of MHD flows have stimulated considerable interest due to its important physical applications in solar physics, meteorology, power generating systems, aeronautics and missile aerodynamics, cosmic fluid dynamics and in the motion of Earth's core, Cramer and Pai [1]. In a broader sense, MHD has applications in three different subject areas, such as astrophysical, geophysical and engineering problems. In light of these applications, free convection about a vertical flat plate embedded in a porous medium with application to heat transfer from a dike, has been studied by Cheng and Minkowycz [2]. The effect of slip condition on MHD steady flow in a channel with permeable boundaries has been discussed by Makinde and Osalusi [3]. Makinde and Mhone [4] investigated on the heat transfer to MHD oscillatory flow in a channel filled with porous medium. Venkateswarlu et al. [5-8] studied the heat and mass transfer effects on unsteady radiative MHD natural convective flow past an infinite vertical porous plate. Recently Turkyimazoglu and Pop [9] investigated analytically Soret and heat source effects on the unsteady radiative MHD free convection flow from an impulsively started infinite vertical plate.

The heat transfer enhancement is one of the most important technical aims for engineering systems due to its wide applications in electronics, cooling systems, post accident heat removal, fire and combustion modelling, development of metal waste from spent nuclear fuel, next-generation solar film collectors, heat exchangers technology, applications in the field of nuclear energy and various thermal systems. Sparrow and Cess [10] were one of the initial investigators to consider temperature dependent heat absorption on steady stagnation point flow and heat transfer. Ishak [11] worked mixed convection boundary layer flow over a horizontal plate with thermal radiation. Analytical solutions for hydromagnetic free convection of a particulate suspension from an inclined plate with heat absor-ption were presented by Ramadan and Chamkha [12]. Venkateswarlu et al. [13-16] investigated the Soret and chemical reaction effects on the radiative MHD flow from an infinite vertical porous plate.

The following strategy is pursued in the rest of the paper. Section two presents the formation of the problem. The analytical solutions are presented in section three. Results are discussed in section four and finally section five provi-des a conclusion of the paper.

2. Formation of the problem

We consider the unsteady laminar slip flow of an incompressible, viscous and electrically conducting fluid through a channel with non-uniform wall temperature bounded by two parallel plates separated by a distance h. The channel is assumed to be filled with a saturated porous medium. A uniform magnetic field of strength B_o is applied perpendicular to the plates. The above plate is heated at constant temperature. It is assumed that there exist a homogeneous chemical reaction of first order with constant rate K_r^* between the diffusing species and the fluid. Initially i.e. at time $t \leq 0$, both the fluid and plate are at rest and at uniform temperature T_o. Also species concentration within the fluid is maintained at uniform concentration C_o .Geometry of the problem is presented in Fig. 1. We choose a Cartesian coordinate system (x, y) where $x-$lies along the centre of the channel, $y-$ is the distance measured in the normal section such that $y = h$ is the channel's width as shown in the figure below. Under the usual Bousinesq approximation, the equations governing the flow can be written as (see, Adesanya and Makinde [17]):

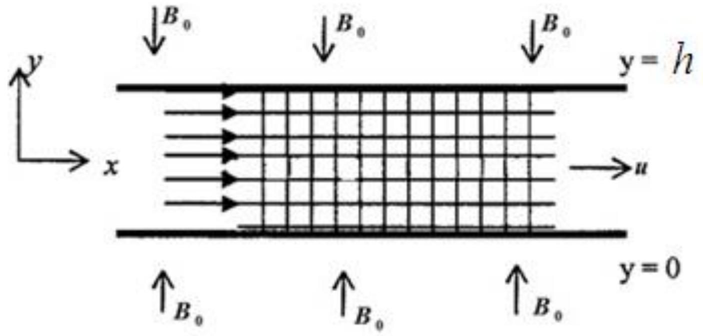

Fig.1: Geometry of the problem

Continuity equation:

$$\frac{\partial v}{\partial y}=0 \tag{1}$$

Momentum equation:

$$\frac{\partial u}{\partial t}=-\frac{1}{\rho}\frac{dp}{dx}+\nu\frac{\partial^2 u}{\partial y^2}+g\beta_T\left(T-T_0\right)+g\beta_C\left(C-C_0\right)-\frac{\sigma_e B_0^2}{\rho}u-\frac{\nu}{K}u \tag{2}$$

Energy equation:

$$\frac{\partial T}{\partial t}=\frac{K_T}{\rho c_p}\frac{\partial^2 T}{\partial y^2}-\frac{Q_o}{\rho c_p}\left(T-T_0\right) \tag{3}$$

Concentration equation:

$$\frac{\partial C}{\partial t}=D_m\frac{\partial^2 C}{\partial y^2}+\frac{D_m K_T}{T_m}\frac{\partial^2 T}{\partial y^2}-K_r^*\left(C-C_0\right) \tag{4}$$

Assuming that slipping occurs between the plate and fluid, the corresponding initial and boundary conditions of the system of partial differential equations for the fluid flow problem are given below

$$\left.\begin{aligned} &u=\phi_1\frac{du}{dy},\quad T=T_0,\quad C=C_0 \quad at \quad y=0\\ &u=\phi_2\frac{du}{dy}, T=T_1+\varepsilon\left(T_1-T_o\right)exp\left(int\right), C=C_1+\varepsilon\left(C_1-C_o\right)exp\left(int\right)\ at\ y=a \end{aligned}\right\} \tag{5}$$

where $n-$ frequency of oscillation and $\varepsilon<<1$ is a very small positive constant.
we introduce the following non-dimensional variables

$$\psi=\frac{x}{h},\eta=\frac{y}{h},U=\frac{h}{\nu}u,\ P=\frac{h^2}{\rho\nu^2}p,\gamma=\frac{\phi_1}{h},\sigma=\frac{\phi_2}{h},\omega=\frac{h^2}{\nu}n,\tau=\frac{\nu}{h^2}t,\theta=\frac{T-T_o}{T_1-T_o},\phi=\frac{C-C_o}{C_1-C_o} \tag{6}$$

Equations (2), (3) and (4) reduce to the following non-dimensional form

$$\frac{\partial U}{\partial\tau}=-\frac{dP}{d\psi}+\frac{\partial^2 U}{\partial\eta^2}+Gr\theta+Gm\phi-\left[M+\frac{1}{Da}\right]U \tag{7}$$

$$\frac{\partial\theta}{\partial\tau}=\frac{1}{Pr}\frac{\partial^2\theta}{\partial\eta^2}-H\theta \tag{8}$$

$$\frac{\partial\phi}{\partial\tau}=\frac{1}{Sc}\frac{\partial^2\phi}{\partial\eta^2}+Sr\frac{\partial^2\theta}{\partial\eta^2}-Kr\phi \tag{9}$$

Here $Gr=\frac{g\beta_T\left(T_1-T_o\right)h^3}{\nu^2}$ is the thermal buoyancy force, $Gm=\frac{g\beta_C\left(C_1-C_0\right)h^3}{\nu^2}$ is the concentration buoyancy force, $M=\frac{\sigma_e B_o^2 h^2}{\rho\nu}$ is the magnetic parameter, $Da=\frac{K}{h^2}$ is the Darcy parameter, $Pr=\frac{\rho c_p\nu}{K_T}$ is the Prandtl number, $H=\frac{Q_0 h^2}{\rho c_p\nu}$ is the heat source parameter, $Sr=\frac{D_m K_T\left(T_1-T_o\right)}{T_m\nu\left(C_1-C_0\right)}$ is the Soret number, $Sc=\frac{\nu}{D_m}$ is the Schmidt number and

$Kr = \frac{h^2}{\nu} K_r^*$ is the chemical reaction parameter respectively.

Initial and boundary conditions, in non-dimensional form, are given by

$$\left.\begin{aligned} &U = \gamma \frac{dU}{d\eta}, \quad \theta = 0, \quad \phi = 0 \text{ at } \eta = 0 \\ &U = \sigma \frac{dU}{d\eta}, \theta = 1 + \varepsilon \exp(i\omega\tau), \phi = 1 + \varepsilon \exp(i\omega\tau) \text{ at } \eta = 1 \end{aligned}\right\} \tag{10}$$

Following Adesanya and Makinde[17],for purely an oscillatory flow we take the pressure gradient of the form

$$\lambda = -\frac{dP}{d\psi} = \lambda_o + \varepsilon \exp(i\omega t)\lambda_1 \tag{11}$$

where λ_o – and λ_1 – are constants and ω is the frequency of oscillation.

Given the velocity, temperature and concentration fields in the boundary layer, the shear stress τ_w, the heat flux q_w and mass flux j_w are obtained by

$$\tau_w = \mu \left[\frac{\partial u}{\partial y}\right], \qquad q_w = -K_T \left[\frac{\partial T}{\partial y}\right], \qquad j_w = -D_m \left[\frac{\partial C}{\partial y}\right] \tag{12}$$

In non-dimensional form the skin-friction coefficient Cf, heat transfer coefficient Nu and mass transfer coefficient Sh are defined as

$$Cf = \frac{\tau_w}{\rho(\nu/h)^2}, \qquad Nu = \frac{hq_w}{K_T(T_1 - T_o)}, \qquad Sh = \frac{hj_w}{D_m(C_1 - C_o)} \tag{13}$$

Using non-dimensional variables in equation (6) and equation (12)) in equation (13), we obtain the physical parameters

$$Cf = \left[\frac{\partial U}{\partial \eta}\right], \qquad Nu = -\left[\frac{\partial \theta}{\partial \eta}\right], \qquad Sh = -\left[\frac{\partial \phi}{\partial \eta}\right] \tag{14}$$

3. Solution of the problem

We assume the trial solutions for velocity, temperature and concentration of the fluid as (see, Venkateswarlu et al. [18-19] and Siva Kumar et al. [20]):

$$U(\eta,\tau) = U_0(\eta) + \varepsilon \exp(i\omega\tau) U_1(\eta) + o(\varepsilon^2) \tag{15}$$

$$\theta(\eta,\tau) = \theta_0(\eta) + \varepsilon \exp(i\omega\tau) \theta_1(\eta) + o(\varepsilon^2) \tag{16}$$

$$\phi(\eta,\tau) = \phi_0(\eta) + \varepsilon \exp(i\omega\tau) \phi_1(\eta) + o(\varepsilon^2) \tag{17}$$

Substituting equations (15) – (17) into equations (7) – (9), then equating the harmonic and non–harmonic terms and neglecting the higher order terms of $o(\varepsilon^2)$, we obtain

$$U_0'' - \left[M + \frac{1}{Da}\right] U_0 = -\left[Gr\theta_0 + Gm\phi_0 + \lambda_0\right] \tag{18}$$

$$U_1'' - \left[M + \frac{1}{Da} + i\omega \right] U_1 = -\left[Gr\theta_1 + Gm\phi_1 + \lambda_1 \right] \quad (19)$$

$$\theta_0'' - Pr\, H\theta_0 = 0 \quad (20)$$

$$\theta_1'' - Pr\left(H + i\omega\right)\theta_1 = 0 \quad (21)$$

$$\phi_0'' - ScKr\phi_0 = -ScSr\theta_o'' \quad (22)$$

$$\phi_1'' - Sc\left(Kr + i\omega\right)\phi_1 = -ScSr\theta_1'' \quad (23)$$

where the prime denotes the ordinary differentiation with respect to η.

Initial and boundary conditions, presented by equation (10), can be written as

$$\left.\begin{array}{l} U_o = \gamma \dfrac{dU_o}{d\eta}, \quad U_1 = \gamma \dfrac{dU_1}{d\eta}, \quad \theta_o = 0, \theta_1 = 0, \quad \phi_o = 0, \quad \phi_1 = 0 \quad \text{at} \quad \eta = 0 \\ U_o = \sigma \dfrac{dU_o}{d\eta}, \quad U_1 = \sigma \dfrac{dU_1}{d\eta}, \quad \theta_o = 1, \theta_1 = 1, \quad \phi_o = 1, \quad \phi_1 = 1 \quad \text{at} \quad \eta = 1 \end{array}\right\} \quad (24)$$

The analytical solutions of equations (18) – (23) with the boundary conditions in equation (24), are given by

$$U_o = A_{22}\exp\left(-m_5\eta\right) + A_{21}\exp\left(m_5\eta\right) + A_8 + \frac{A_6\sinh(m_1\eta)}{\sinh(m_1)} - \frac{A_7\sinh(m_3\eta)}{\sinh(m_3)} \quad (25)$$

$$U_1 = A_{39}\exp\left(-m_6\eta\right) + A_{38}\exp\left(m_6\eta\right) + A_{25} + \frac{A_{23}\sinh(m_2\eta)}{\sinh(m_2)} - \frac{A_{24}\sinh(m_4\eta)}{\sinh(m_4)} \quad (26)$$

$$\theta_o = \frac{\sinh(m_1\eta)}{\sinh(m_1)} \quad (27)$$

$$\theta_1 = \frac{\sinh(m_2\eta)}{\sinh(m_2)} \quad (28)$$

$$\phi_o = \frac{A_3\sinh(m_3\eta)}{\sinh(m_3)} - \frac{A_2\sinh(m_1\eta)}{\sinh(m_1)} \quad (29)$$

$$\phi_1 = \frac{A_5\sinh(m_4\eta)}{\sinh(m_4)} - \frac{A_4\sinh(m_2\eta)}{\sinh(m_2)} \quad (30)$$

By substituting equations (25) – (30) into equations (15) – (17), we obtained solutions for the fluid velocity, temperature and concentration and are presented in the following form

$$\begin{array}{l} U\left(\eta,\tau\right) = \left[A_{22}\exp\left(-m_5\eta\right) + A_{21}\exp\left(m_5\eta\right) + A_8 + \dfrac{A_6\sinh(m_1\eta)}{\sinh(m_1)} - \dfrac{A_7\sinh(m_3\eta)}{\sinh(m_3)} \right] + \\ \varepsilon\exp\left(i\omega\tau\right)\left[A_{39}\exp\left(-m_6\eta\right) + A_{38}\exp\left(m_6\eta\right) + A_{25} + \dfrac{A_{23}\sinh(m_2\eta)}{\sinh(m_2)} - \dfrac{A_{24}\sinh(m_4\eta)}{\sinh(m_4)} \right] \end{array} \quad (31)$$

$$\theta\left(\eta,\tau\right) = \left[\frac{\sinh(m_1\eta)}{\sinh(m_1)} \right] + \varepsilon\exp\left(i\omega\tau\right)\left[\frac{\sinh(m_2\eta)}{\sinh(m_2)} \right] \quad (32)$$

$$\phi\left(\eta,\tau\right) = \left[\frac{A_3\sinh(m_3\eta)}{\sinh(m_3)} - \frac{A_2\sinh(m_1\eta)}{\sinh(m_1)} \right] + \varepsilon\exp\left(i\omega\tau\right)\left[\frac{A_5\sinh(m_4\eta)}{\sinh(m_4)} - \frac{A_4\sinh(m_2\eta)}{\sinh(m_2)} \right] \quad (33)$$

3.1 Skin friction: From the velocity field, the skin friction coefficient at the plate can be obtained, which in non dimensional form is given by

$$Cf = \left[A_{21} m_5 \exp(m_5\eta) - m_5 A_{22} \exp(-m_5\eta) + \frac{A_6 m_1 \cosh(m_1\eta)}{\sinh(m_1)} - \frac{A_7 m_3 \cosh(m_3\eta)}{\sinh(m_3)} \right] + \varepsilon \exp(i\omega\tau) \left[A_{38} m_6 \exp(m_6\eta) - A_{39} m_6 \exp(-m_6\eta) + \frac{A_{23} m_2 \cosh(m_2\eta)}{\sinh(m_2)} - \frac{A_{24} m_4 \cosh(m_4\eta)}{\sinh(m_4)} \right] \quad (34)$$

3.2 Nusselt number: From the temperature field, we obtained the rate of heat transfer coefficient which is given in non-dimensional form as

$$Nu = -\left[\frac{m_1 \cosh(m_1\eta)}{\sinh(m_1)} \right] - \varepsilon \exp(i\omega\tau) \left[\frac{m_2 \cosh(m_2\eta)}{\sinh(m_2)} \right] \quad (35)$$

3. 3 Sherwood number: From the concentration field, we obtained the rate of mass transfer coefficient which is given in non-dimensional form as

$$Sh = \left[\frac{A_2 m_1 \cosh(m_1\eta)}{\sinh(m_1)} - \frac{A_3 m_3 \cosh(m_3\eta)}{\sinh(m_3)} \right] + \varepsilon e^{i\omega\tau} \left[\frac{A_4 m_2 \cosh(m_2\eta)}{\sinh(m_2)} - \frac{A_5 m_4 \cosh(m_4\eta)}{\sinh(m_4)} \right] \quad (36)$$

Here $m_1 = \sqrt{\Pr H}, m_2 = \sqrt{\Pr(H + i\omega)}, m_3 = \sqrt{ScKr}, m_4 = \sqrt{Sc(Kr + i\omega)}, m_5 = \sqrt{M + \frac{1}{Da}},$

$m_6 = \sqrt{M + \frac{1}{Da} + i\omega}, A_1 = ScSr,\ A_2 = \frac{m_1^2 A_1}{m_1^2 - m_3^2},\quad A_3 = 1 + A_2,\quad A_4 = \frac{m_2^2 A_1}{m_2^2 - m_4^2},\quad A_5 = 1 + A_4,$

$A_6 = \frac{GmA_2 - Gr}{m_1^2 - m_5^2}, A_7 = \frac{GmA_3}{m_3^2 - m_5^2}, A_8 = \frac{\lambda_0}{m_5^2}, A_9 = \frac{\gamma m_1 A_6}{\sinh(m_1)}, A_{10} = \frac{\gamma m_3 A_7}{\sinh(m_3)}, A_{11} = A_9 - (A_8 + A_{10}),$

$A_{12} = A_6 [\sigma m_1 \coth(m_1) - 1],\ A_{13} = A_7 [\sigma m_3 \coth(m_3) - 1],\ A_{14} = A_{12} - (A_8 + A_{13}),\ A_{15} = 1 + \gamma m_5,$

$A_{16} = 1 - \gamma m_5,\quad A_{17} = 1 + \sigma m_5,\quad A_{18} = 1 - \sigma m_5,\quad A_{19} = A_{16} A_{17} \exp(-m_5) - A_{15} A_{18} \exp(m_5),$

$A_{20} = A_{11} A_{17} \exp(-m_5) - A_{14} A_{15}, A_{21} = \frac{A_{20}}{A_{19}}, A_{22} = \frac{A_{11} - A_{16} A_{21}}{A_{15}}, A_{23} = \frac{GmA_4 - Gr}{m_2^2 - m_6^2}, A_{24} = \frac{GmA_5}{m_4^2 - m_6^2},$

$A_{25} = \frac{\lambda_1}{m_6^2}, A_{26} = \frac{\gamma m_2 A_{23}}{\sinh(m_2)}, A_{27} = \frac{\gamma m_4 A_{24}}{\sinh(m_4)}, A_{28} = A_{26} - (A_{25} + A_{27}), A_{29} = A_{23} [\sigma m_2 \coth(m_2) - 1],$

$A_{30} = A_{24} [\sigma m_4 \cot(m_4) - 1],\ A_{31} = A_{29} - (A_{25} + A_{30}),\ A_{32} = 1 + \gamma m_6, A_{33} = 1 - \gamma m_6, A_{34} = 1 + \sigma m_6,$

$A_{35} = 1 - \sigma m_6,\quad A_{36} = A_{33} A_{34} \exp(-m_6) - A_{32} A_{35} \exp(m_6),\quad A_{37} = A_{28} A_{34} \exp(-m_6) - A_{31} A_{32},$

$A_{38} = \frac{A_{37}}{A_{36}}, A_{39} = \frac{A_{28} - A_{33} A_{38}}{A_{32}}$

4. Results and discussion

In order to obtain the physical significance of the problem, we have plotted the fluid velocity, temperature and concentration for different values of physical parameters. The numerical values of the skin friction coefficient, the rate of heat transfer coefficient and the rate of mass transfer coefficient are presented in tabular form for varies values of physical parameters. In the present study following default parameter values are adopted for computations: $\tau = \pi / 2, \lambda = 0.5,$ $Gr = 5, Gm = 5, M = 2, Da = 1, \gamma = 0.1, \sigma = 0.1, \Pr = 0.71, H = 5, Sc = 0.78, Sr = 5, Kr = 0.5,$ $\omega = 1, \varepsilon = 0.001.$ Hence all the graphs and tables are corresponding to these values unless specifically indicated on the appropriate graph or table.

The effects of thermal Grashof number Gr and solutal Grashof number Gm on the velocity U of the flow field are presented in Figs. 2 and 3. Physically, thermal Grashof number Gr signifies the relative strength of thermal buoyancy force to viscous hydrodynamic force in the boundary layer. Solutal Grashof number Gm signifies the relative strength of species buoyancy force to viscous hydrodynamic force in the boundary layer. A study of the curves shows that thermal Grashof number Gr and solutal Grashof number Gm accelerates the velocity of the flow field at all points. This is due to the reason that there is an enhancement in thermal buoyancy force and concentration buoyancy force.

Fig.4 shows the variation of fluid velocity U with the Darcy parameter Da. The graph shows that an increase in the Darcy parameter increases the fluid flow except at the flow reversal points at the heated wall. Fig. 5 depicts the influence of pressure gradient λ on the fluid velocity U. It is observed that, the fluid velocity U increases on increasing the pressure gradient λ. Fig.6 depicts the influence of magnetic field intensity on the variation of fluid velocity. It is noticed that, an increase in the magnetic parameter M decreases the fluid velocity U due to the resistive action of the Lorenz forces except at the heated wall where the reversed flow induced by wall slip caused an increase in the fluid velocity. This implies that magnetic field tends to decelerate fluid flow.

Figs. 7 and 8 shows the fluid velocity profile variations with the cold wall slip parameter γ and the heated wall slip parameter σ. It is observed that, the fluid velocity U increases on increasing the cold wall slip parameter γ thus enhancing the fluid flow. The cold wall slip parameter did not cause any appreciable effect on the heated wall. An increase in the heated wall slip parameter σ decreases the fluid velocity minimally at the cold wall and increasing the heated wall slip parameter causes a flow reversal towards the heated wall. It is observed that $\sigma = 0$ corresponds to the pulsatile case with no slip condition at the heated wall in Fig 8.

Figs. 9 to 11, demonstrate the plot of fluid velocity U, temperature θ and concentration ϕ for a variety of heat source parameter H. It is seen that, the fluid velocity and concentration increases on increasing the heat source parameter whereas temperature decreases on increasing the heat source parameter. This implies that heat source tend to accelerate the fluid velocity and concentration whereas it has a reverse effect on temperature.

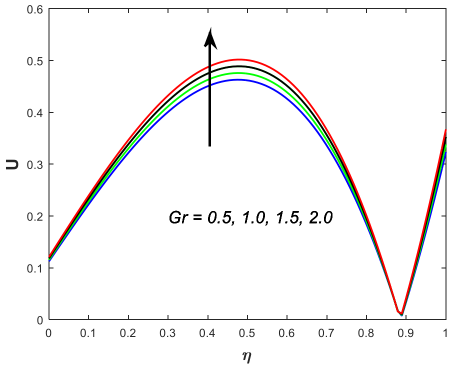

Fig. 2: Influence of Grashof number on velocity profiles.

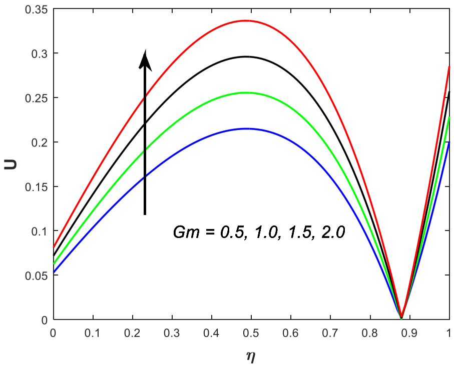

Fig. 3: Influence of solutalGrashof number on velocity profiles.

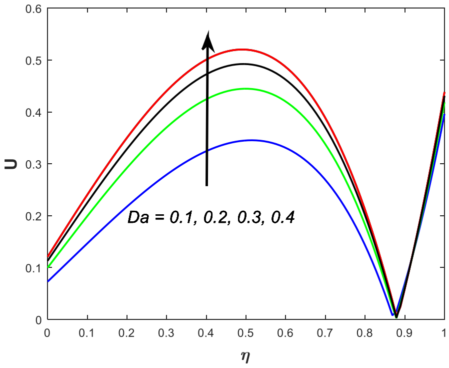

Fig. 4: Influence of Darcy parameter on velocity profiles.

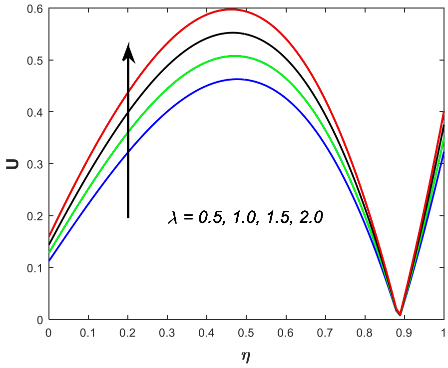

Fig. 5: Influence of pressure gradient on velocity profiles.

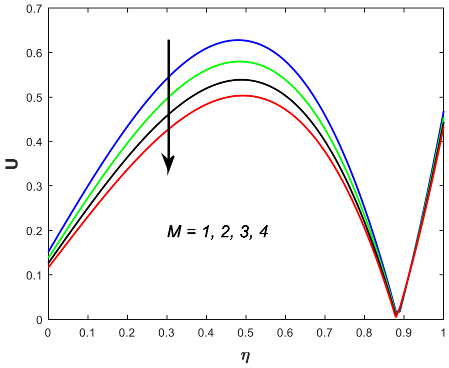

Fig. 6: Influence of magnetic parameter on velocity profiles.

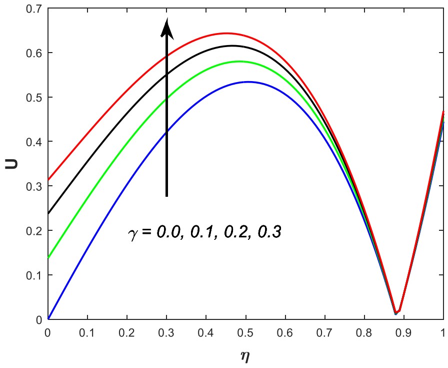

Fig. 7: Influence of cold wall slip parameter on velocity profiles.

Figs. 12 to 14, shows the plot of fluid velocity U, temperature θ and concentration ϕ of the flow field against different values of Prandtl number Pr. Prandtl number defines the ratio of momentum diffusivity to thermal diffusivity. It is evident, that the velocity U and concentration ϕ increases on increasing Prandtl number Pr whereas temperature θ decreases on increasing Pr. Thus higher Prandtl number leads to faster cooling of the plate. This is because radiation and heat source have tendency to reduce fluid temperature.

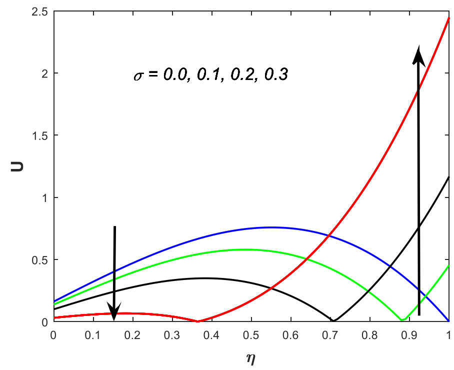

Fig. 8: Influence of heated wall slip parameter on velocity profiles.

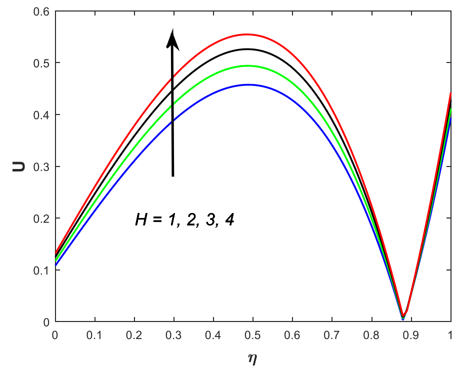

Fig. 9: Influence of heat source parameter on velocity profiles.

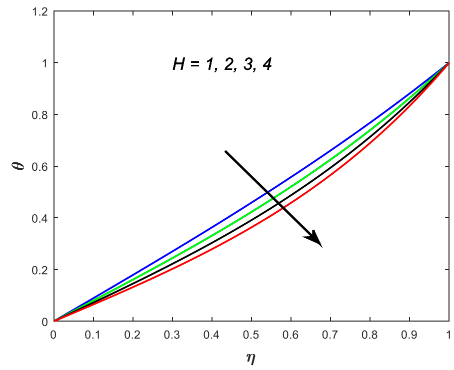

Fig. 10: Influence of heat source parameter on temperature profiles.

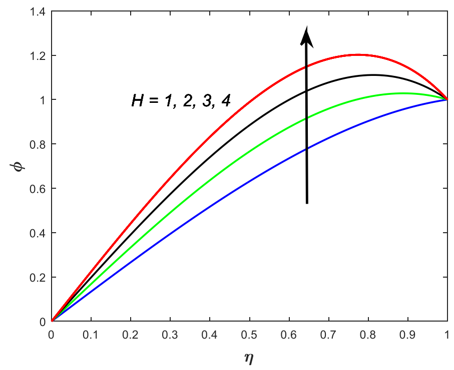

Fig. 11: Influence of heat source parameter on concentration profiles.

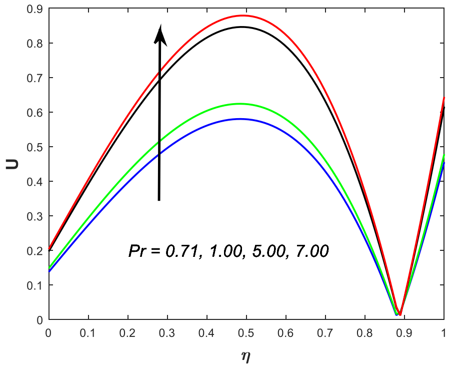

Fig. 12: Influence of Prandtl number on velocity profiles

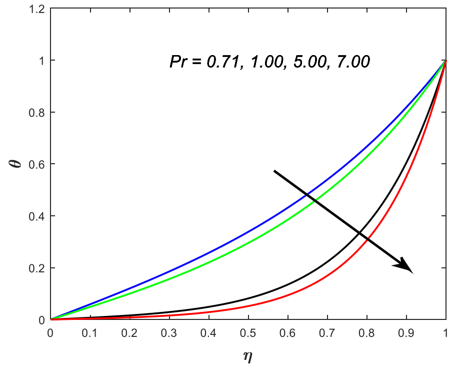

Fig. 13: Influence of Prandtl number on temperature profiles.

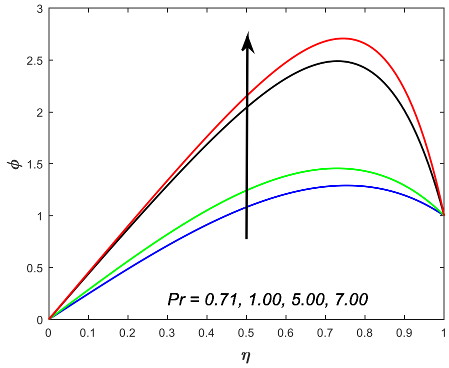

Fig. 14: Influence of Prandtl number on concentration profiles.

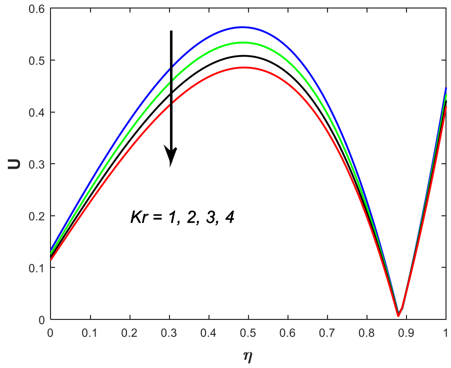

Fig. 15: Influence of chemical reaction parameter on velocity profiles.

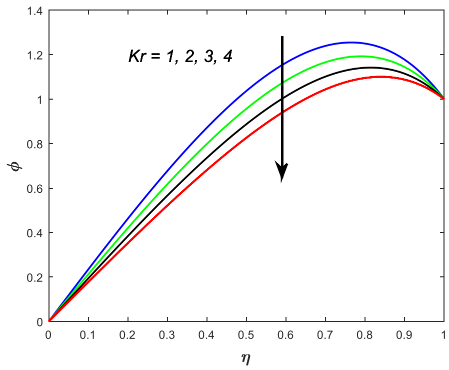

Fig. 16: Influence of chemical reaction parameter on concentration profiles.

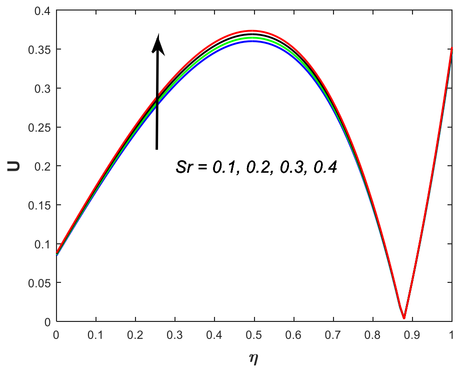

Fig. 17: Influence of Soret number on velocity profiles.

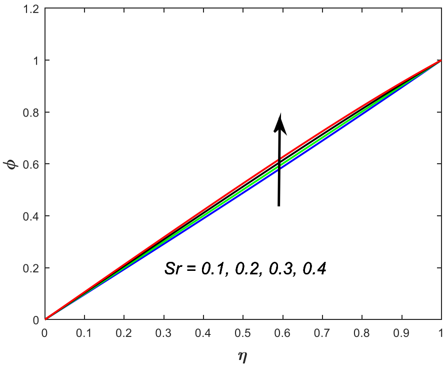

Fig. 18: Influence of Soret number on concentration profiles.

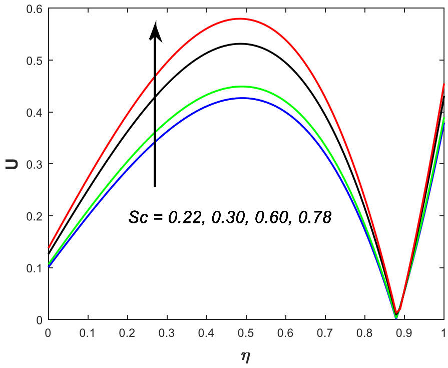

Fig. 19: Influence of Schmidt number on velocity profiles.

Figs. 15 and 16 demonstrate the effects of chemical reaction parameter Kr on the velocity and species concentration. It is observed that, both velocity U and species concentration ϕ decreases on increasing the chemical reaction parameter Kr. Figs. 17 and 18 depict the influence of Soret number Sr on the fluid velocity U and species concentration ϕ of the flow field. It is noticed that, velocity U and species concentration ϕ is found to increases on increasing the Soret number Sr.

The nature of velocity U in presence of foreign species such as Hydrogen $(Sc = 0.22)$, Helium $(Sc = 0.30)$, Water vapour $(Sc = 0.60)$, Ammonia $(Sc = 0.78)$ is shown in Fig. 19. Physically, Schmidt number Sc signifies the relative strength of viscosity to chemical molecular diffusivity. It is observed that U increases on increasing Sc. The flow field enhances the fluid velocity U in presence of heavier diffusing species.

The numerical values of skin friction Cf are presented in tabular form in tables 1 to 3. It is clear that, the skin friction Cf increases on increasing the thermal Grashof number Gr, solutal Grashof number Gm, Darcy parameter Da, pressure gradient λ, Prandtl number Pr, heat source parameter H, Schmidt number Sc and Soret number Sr whereas it decreases on increasing the magnetic parameter M and chemical reaction parameter Kr at both cold and heated plates. Skin friction coefficient decreases at the cold plate but increases at the heated plate with an increase in the cold wall slip parameter γ and heated wall slip parameter σ.

The numerical values of the heat transfer coefficient Nu are presented in tabular form in table 4. It is clear that, the Nusselt number Nu increases at the cold plate but decreases at the heated plate on increasing the Prandtl number Pr and heat source parameter H.

Table 1

Effect of Gr, Gm, M and Da on skin friction coefficient

Gr	Gm	M	Da	Skin friction Cf	
				Cold wall	Heated wall
0.5	5.0	2.0	1.0	1.1254	3.2337
1.0	5.0	2.0	1.0	1.1533	3.3799
1.5	5.0	2.0	1.0	1.1812	3.5261
2.0	5.0	2.0	1.0	1.2091	3.6723
5.0	0.5	2.0	1.0	0.5297	2.0046
5.0	1.0	2.0	1.0	0.6238	2.2874
5.0	1.5	2.0	1.0	0.7179	2.5702
5.0	2.0	2.0	1.0	0.8119	2.8530
5.0	5.0	1.0	1.0	1.5135	4.6864
5.0	5.0	2.0	1.0	1.3765	4.5496
5.0	5.0	3.0	1.0	1.2601	4.4349
5.0	5.0	4.0	1.0	1.1602	4.3380
5.0	5.0	2.0	0.1	0.7287	3.9631
5.0	5.0	2.0	0.2	0.9977	4.1856
5.0	5.0	2.0	0.3	1.1300	4.3091
5.0	5.0	2.0	0.4	1.2083	4.3845

Table 2

Effect of λ, γ, σ and Pr on skin friction coefficient

λ	γ	σ	Pr	Skin friction Cf	
				Cold wall	Heated wall
0.5	0.1	0.1	0.71	1.3765	4.5496
1.0	0.1	0.1	0.71	1.5331	4.8093
1.5	0.1	0.1	0.71	1.6897	5.0690
2.0	0.1	0.1	0.71	1.8463	5.3287
0.5	0.0	0.1	0.71	1.6370	4.4429
0.5	0.1	0.1	0.71	1.3765	4.5496
0.5	0.2	0.1	0.71	1.1875	4.6271
0.5	0.3	0.1	0.71	1.0441	4.6859
0.5	0.1	0.0	0.71	1.6196	3.7262
0.5	0.1	0.1	0.71	1.3765	4.5496
0.5	0.1	0.2	0.71	0.9955	5.8403
0.5	0.1	0.3	0.71	0.3128	8.1533
0.5	0.1	0.1	0.71	1.3765	4.5496
0.5	0.1	0.1	1.00	1.4797	4.7798
0.5	0.1	0.1	5.00	1.9698	6.1546
0.5	0.1	0.1	7.00	2.0338	6.4379

Table 3

Effect of λ, γ, σ and Pr on skin friction coefficient

H	Sc	Sr	Kr	Skin friction Cf	
				Cold wall	Heated wall
1.0	0.78	5.0	0.5	1.0834	3.9364

2.0	0.78	5.0	0.5	1.1717	4.1161
3.0	0.78	5.0	0.5	1.2487	4.2761
4.0	0.78	5.0	0.5	1.3165	4.4198
5.0	0.22	5.0	0.5	1.0091	3.7890
5.0	0.30	5.0	0.5	1.0630	3.9000
5.0	0.60	5.0	0.5	1.2608	4.3093
5.0	0.78	5.0	0.5	1.3765	4.5496
5.0	0.78	0.1	0.5	0.8484	3.4601
5.0	0.78	0.2	0.5	0.8591	3.4823
5.0	0.78	0.3	0.5	0.8699	3.5045
5.0	0.78	0.4	0.5	0.8807	3.5268
5.0	0.78	5.0	1.0	1.3358	4.4736
5.0	0.78	5.0	2.0	1.2630	4.3363
5.0	0.78	5.0	3.0	1.1999	4.2157
5.0	0.78	5.0	4.0	1.1448	4.1089

The numerical values of the mass transfer coefficient Sh are presented in tabular form in table 5. It is clear that, Sherwood number Sh increases at the cold plate but decreases at the heated plate on increasing the Soret number Sr. Sherwood number Sh decreases at both cold and heated plates with an increase in the chemical reaction parameter Kr. Mass transfer coefficient Sh increases at both cold and heated plates on increasing the Prandtl number Pr, heat source parameter H and Schmidt number Sc.

Table 4

Effect of Pr and H on heat transfer coefficient

Pr	H	Nusselt number Nu	
		Cold wall	Heated wall
0.71	5.0	-0.5862	-1.9731
1.00	5.0	-0.4836	-2.2875
5.00	5.0	-0.0674	-5.0000
7.00	5.0	-0.0319	-5.9156
0.71	1.0	-0.8909	-1.2260
0.71	2.0	-0.7975	-1.4336
0.71	3.0	-0.7170	-1.6259
0.71	4.0	-0.6472	-1.8050

Table 5

Effect of Pr, H, Sc, Sr, and Kr on mass transfer coefficient

Pr	H	Sc	Sr	Kr	Sherwood number Sh	
					Cold wall	Heated wall
0.71	5.0	0.78	5.0	0.5	2.4787	2.5817
1.00	5.0	0.78	5.0	0.5	2.8598	3.7839
5.00	5.0	0.78	5.0	0.5	4.3868	14.2190
7.00	5.0	0.78	5.0	0.5	4.5113	17.7610
0.71	1.0	0.78	5.0	0.5	1.3448	0.2669

0.71	2.0	0.78	5.0	0.5	1.6927	0.5240
0.71	3.0	0.78	5.0	0.5	1.9923	1.2567
0.71	4.0	0.78	5.0	0.5	2.2521	1.9402
0.71	5.0	0.22	5.0	0.5	1.4311	0.0270
0.71	5.0	0.30	5.0	0.5	1.5851	0.3971
0.71	5.0	0.60	5.0	0.5	2.1495	1.7696
0.71	5.0	0.78	5.0	0.5	2.4787	2.5817
0.71	5.0	0.78	0.1	0.5	0.9688	1.0523
0.71	5.0	0.78	0.2	0.5	0.9996	0.9782
0.71	5.0	0.78	0.3	0.5	1.0304	0.9040
0.71	5.0	0.78	0.4	0.5	1.0612	0.8298
0.71	5.0	0.78	5.0	1.0	2.3543	2.3801
0.71	5.0	0.78	5.0	2.0	2.1335	2.0079
0.71	5.0	0.78	5.0	3.0	1.9439	1.6710
0.71	5.0	0.78	5.0	4.0	1.7798	1.3632

5. Conclusions

From the present investigation the following conclusions can be drawn:

- Cold wall slip parameter, heat source parameter and Soret number are tend to accelerate the fluid velocity whereas magnetic parameter and chemical reaction parameter have a reverse effect on it. Increasing heated wall slip parameter causes a flow reversal towards the heated plate.
- Heat source parameter and Prandtl number are tending to retard the fluid temperature.
- Heat source parameter and Soret number and are tend to accelerate the species concentration whereas chemical reaction parameter has a reverse effect on it.
- Heat source parameter and Soret number are tends to accelerate the skin friction whereas magnetic parameter and chemical reaction parameter have a reverse effect on it at both cold and heated plates. Skin friction decreases at the cold plate but increases at the heated the plate on increasing the cold wall slip parameter and heated wall slip parameter.
- Heat transfer coefficient increases at the cold plate but decreases at the heated plate on increasing the heat source parameter and Prandtl number.
- Mass transfer coefficient increases at both cold and heated plates on increaseing the heat source parameter and Schmidt number where as chemical reaction parameter has a reverse effect on it. Soret number accelerates the mass transfer coefficient at the cold plate whereas it has a reverse effect at the heated plate.

Acknowledgements

Authors are thankful for the suggestions and comments of the referees, which have led to improvement of the paper.

R E F E R E N C E S

[1] *K. R. Cramer and S. I. Pai:* Magnetofluid dynamics for engineers and applied physicists, Mc Graw Hill Book Company, New York, 1973.

[2] *P. Cheng and W. J. Minkowycz:* Free convection about a vertical flat plate embedded in a porous medium with application to heat transfer from a dike, J. Geophys. Res.,vol. 82, no. 14, 1977, pp. 2040-2044.

[3] *O. D. Makinde and E. Osalusi:* MHD Steady flow in a channel with slip at the permeable boundaries, Rom. J. Phys, vol. 51, 2006, pp. 319–328.

[4] *O. D. Makinde and P. Y. Mhone:* Heat transfer to MHD oscillatory flow in a channel filled with porous medium, Rom. J. Phys, vol. 50, 2005, pp. 931–938.

[5] *Malapati Venkateswarlu and Dasari Venkata Lakshmi:* Thermal diffusion, hall currentand chemical reaction effects on unsteady MHD natural convective flow past a vertical plate, U. P. B. Sci. Bull., Series D: Mechanical Engineering., vol.79, no. 1,2017, pp. 91- 106.

[6] *M. Venkateswarlu, G. V Ramana Reddy and D. V. Lakshmi:* Radiation and chemical reaction effects on MHD flow past an oscillating vertical porous plate with constant heat flux, International Conference on Mathematical Sciences, ISBN–978-93-5107-261-4, 2014, pp. 323-327.

[7] *M. Venkateswarlu, G. V. Ramana Reddy and D. V. Lakshmi:* Thermal diffusion and radiation effects on unsteady MHD free convection heat and mass transfer flow past a linearly accelerated vertical porous plate with variable temperature and mass diffusion, J. Korean Soc. Ind. Appl. Math., vol.18, no.3,2014, pp. 257-268.

[8] *M. Venkateswarlu, G. V. Ramana Reddy and D. V. Lakshmi:* Radiation effects on MHD boundary layer flow of liquid metal over a porous stretching surface in porous medium with heat generation, J. Korean Soc. Ind. Appl. Math., vol. 19, no. 1, 2015,pp. 83-102.

[9] *M. Turkyimazoglu and I. Pop:* Soret and heat source effects on the unsteady radiative MHD free convection flow from an impulsively started infinite vertical plate, Int. J. Heat and Mass Transf., vol. 55, 2012, pp. 7635–7644.

[10] *E. M. Sparrow and R. D. Cess:* Temperature dependent heat sources or sinks in a stagnation point flow, Appl. Sci. Res., vol. 10, 1961, pp. 185-197.

[11] *A. Ishak:* Mixed convection boundary layer flow over a horizontal plate with thermal radiation, Heat and Mass Transfer., vol. 46, 2009, pp.147–151.

[12] *H. Ramadan and A. J. Chamkha:* Analytical solutions for hydromagnetic free convection of a particulate suspension from an inclined plate with heat absorption, Int. J. Fluid Mech. Res., vol. 27, 2004,pp. 447-467.

[13] *Venkateswarlu Malapati ,Venkata Lakshmi Dasari:* Soret and chemical reaction effects on the radiative MHD flow from an infinite vertical plate, J. Korean Soc. Ind. Appl. Math., vol. 21, no. 1, 2017, pp. 39-61.

[14] *M. Venkateswarlu, G. V. Ramana Reddy and D. V. Lakshmi:* Diffusion-thermo effects on MHD flow past an infinite vertical porous plate in the presence of radiation and chemical reaction, International Journal of Mathematical Archive, vol. 4, no. 9, 2013, pp. 39-51.

[15] *M. Venkateswarlu, G. V. Ramana Reddy and D. V. Lakshmi:* Effects of chemical reaction and heat generation on MHD boundary layer flow of a moving vertical plate with suction and dissipation, Engineering International, vol. 1, no. 1,2013, pp.27-38.

[16] *M. Venkateswarlu, G. V. Ramana Reddy and D. V. Lakshmi*: Unsteady MHD flow of a viscous fluid past a vertical porous plate under oscillatory suction velocity, Advances in Applied Science Research**,** vol. 4, no.6, 2013, pp. 52-67.

[17] *S. O. Adesanya and O. D. Makinde:* MHD oscillatory slip flow and heat transfer in a channel filled with porous media, U.P.B. Sci. Bull., Series A, vol. 76, no. 1, 2014, pp.197-204.

[18] *M. Venkateswarlu and D. Venkata Lakshmi*: Dufour and chemical reaction effects on unsteady MHD flow of a viscous fluid in a parallel porous plate channel under the influence of slip condition, Journal of the Nigerian Mathematical Society, vol. 36, no. 2, 2017, pp. 369-397.

[19] *Venkateswarlu Malapati and Padma polarapu:* Unsteady MHD free convective heat and mass transfer in a boundary layer flow past a vertical permeable plate with thermal radiation and chemical reaction, Procedia Engineering, vol.127, 2015, pp. 791-799.

[20] *N. Siva Kumar, Rushi Kumar and A. G. Vijaya Kumar:* Thermal diffusion and chemical reaction effects on unsteady flow past a vertical porous plate with heat source dependent in slip flow regime, Journal of Naval Architecture and Marine Engineering, vol. 13, 2016,pp. 51-62.